

Numerical Simulation of Ultrasonic Nondestructive Testing for Adhesively Bonded Lap Joints

Xinchao Liu¹, Yifeng Wang^{1,2}, Zhaonan Liu^{1,2}, Xiao Liu¹, Chuck Zhang^{1,2}

1. H. Milton Stewart School of Industrial and Systems Engineering, Georgia Tech, Atlanta, GA, USA.

2. Georgia Tech Manufacturing Institute, Georgia Tech, Atlanta, GA, USA.

Abstract

Nondestructive inspection (NDI) of damages (e.g., imperfect or degraded bondlines) or the remaining strength of adhesively bonded lap joints is critical for the manufacturing and operation of aircrafts, vehicles and wind turbine blades. It remains a challenge to use the conventional NDI to quantitatively infer the poor adhesion between the adherend and the adhesive. Essentially, the direct NDI measurements were related to the latent parameters indicating bond integrity in many studies. Our work is to build a physics-based simulation model of NDI for adhesively bonded lap joints in *COMSOL Multiphysics* by incorporating latent spring-like interfaces between the adherend and the adhesive. The physics interfaces used in the NDI simulation include *Solid Mechanics (Wave)*, *Electrostatics (Piezoelectricity)* and *Electrical Circuit*. The Multiphysics coupling enables modeling both single transducer probes and phased array probes. In this study, we are modeling transducers with wedges. An absorbing layer is defined on the top of the transducer. The NDI model can be either global (e.g., full-size) or local. For computational efficiency, we built a local NDI model assuming periodic boundaries to mimic the pulse-echo-like wave propagation across transducer, wedge, adherend and adhesive. The imperfect bonding interfaces between the adherend and adhesive are modeled as thin elastic layers that can be represented as spring material in *COMSOL*, i.e., spring-type interfaces. Then the interfacial stiffness matrix (or the damping constants) of the spring-like thin elastic layers is employed to characterize the bonding status, e.g., the infinite interfacial stiffness indicates a perfectly bonding. The simulation model allows investigation of the relationship between interfacial properties and NDI measurements, such as ultrasound reflection coefficients, enabling real-time evaluation of bond integrity. Extensive simulations conducted in *LiveLink™* show that spring-damper-interface enhances the widely adopted spring-interface, paving the road for further theoretical explorations.

Keywords: Ultrasonic Nondestructive Testing; Adhesive Joint.

Introduction

Ultrasound testing of bondline integrity is critical for the manufacturing and operation of aircrafts, vehicles and wind turbine blades. This paper studies the effects of adhesive interfaces on the ultrasonic reflection and transmission characteristics. The ultimate goal of this research is to establish a comprehensive understanding of bond assessment through NDI, enhancing safety and reliability in aerospace, automotive and energy applications.

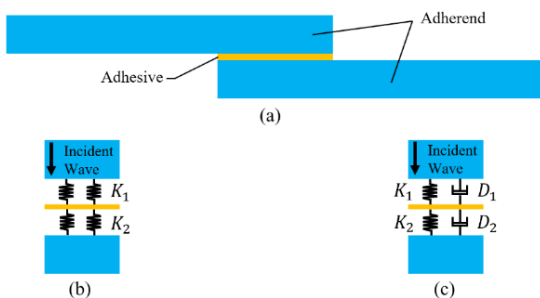


Figure 1. Adhesive lap joints and interfacial characteristics. (a) the adhesive lap joint consisting of two adherends and one adhesive interlayer; (b) spring-interface model; (c) spring-damper-interface model.

Theory / Experimental Set Up

Fig. 1 illustrates the adhesive lap joints and two interface models, i.e., the spring-interface model (Fig. 1b) and the spring-damper-interface model (Fig. 1c). Conventional nondestructive inspection

(NDI) struggles to quantitatively access the poor adhesion between the adherend and the adhesive [1-2]. Previous studies have shown that the direct NDI measurements are related to the latent parameters (e.g., the interfacial stiffness K_1 and K_2) which indicate bond integrity. Our work involves building a physics-based simulation model of NDI for adhesively bonded lap joints using *COMSOL Multiphysics*. This model incorporates spring-like interfaces between the adherend and the adhesive, considering both interfacial stiffness and damping parameters to better represent realistic adhesive bonding interfaces. Extensive simulation runs were performed through *LiveLink™ for MATLAB* to generate ultrasound responses for various adhesive bonding settings. To manage computational demands, this paper focuses on local models (Fig. 1b-c) rather than the global model shown in Fig. 1a. The relationships between ultrasound signals and interfacial characteristics are examined through multiple numerical simulations.

Governing Equations

This study examines pulse-echo-like wave propagation in ultrasound testing. As illustrated in Fig. 1b-c, a normally incident wave is emitted from the probes and then transmitted into adhesive joints. For simplicity, we assume a one-dimensional incident wave propagating along the x-axis. The bulk adherends are semi-definite, homogeneous, and

linear elastic bodies [3]. The elastic wave equation in adherends is described as

$$\frac{\partial^2 u}{\partial t^2} = \frac{1}{\rho} \frac{\partial \sigma}{\partial x} = \frac{1}{\rho} \frac{\partial}{\partial x} \left(\rho c^2 \frac{\partial u}{\partial x} \right) = c^2 \frac{\partial^2 u}{\partial x^2}, \quad (1)$$

where u denotes the displacement with respect to (x, t) , σ is the stress with respect to (x, t) , t represents the time, ρ is the density, and c denotes the wave velocity in the adherend. The Eq. (1) obeys Hooke's law. The adhesive layer shown Fig. 1(a) is homogeneous, elastic bulk body [3]. The thickness of the adhesive layer is denoted as α . According to our applications, we set $\alpha = 0.2 \text{ mm}$ for all simulations in this paper. The density and wave velocity for the adhesive layer are denoted as ρ_0 and c_0 .

The interface boundaries between adherends and adhesive are modeled using both a spring-interface and a spring-damper-interface, as shown in Fig. 1b-c. The spring-interface model without a damper, shown in Figure 1b, is widely used in many studies for ultrasonic weak bond detection. In this study, we extend the model by incorporating a damping parameter into the interface model for ultrasonic transmission and reflection analysis using finite element analysis (FEA). Along the x axis, there are two adherend-adhesive interfaces at $x = 0$ and α . The continuity condition is

$$\begin{aligned} u(0^+, t) &= u(0^-, t), \quad \sigma(0^+, t) = \sigma(0^-, t) \\ u(\alpha^+, t) &= u(\alpha^-, t), \quad \sigma(\alpha^+, t) = \sigma(\alpha^-, t) \end{aligned} \quad (2)$$

where '+' and '-' represent the two sides of $\lim_x u$ and $\lim_x \sigma$ at adherend-adhesive interfaces. For the

spring-interface model, the interface boundaries are

$$\begin{aligned} \sigma(0^+, t) &= \sigma(0^-, t) = K_1 [u(0^+, t) - u(0^-, t)], \\ \sigma(\alpha^+, t) &= \sigma(\alpha^-, t) = K_2 [u(\alpha^+, t) - u(\alpha^-, t)], \end{aligned} \quad (3)$$

where K_1 and K_2 are the interfacial stiffness as shown in Fig. 1(b). For the spring-damper-interface model,

$$\begin{aligned} \sigma(0^+, t) &= \sigma(0^-, t) = K_1 [u(0^+, t) - u(0^-, t)] \\ &\quad + D_1 [\dot{u}(0^+, t) - \dot{u}(0^-, t)], \\ \sigma(\alpha^+, t) &= \sigma(\alpha^-, t) = K_2 [u(\alpha^+, t) - u(\alpha^-, t)] \\ &\quad + D_2 [\dot{u}(\alpha^+, t) - \dot{u}(\alpha^-, t)], \end{aligned} \quad (4)$$

where D_1 and D_2 are the interfacial damping parameters as shown in Fig. 1(c). A perfect adhesive joint is characterized by an infinite interfacial stiffness. Damping is associated with energy dissipation and crack formation in composites, and good damping properties are crucial in the design of composites [4]. Therefore, incorporating damping into the interface model is essential for effective ultrasonic weak bond detection.

Use of Simulation Apps

The physics options used in our NDI simulation include *Solid Mechanics (Wave)*, *Electrostatics (Piezoelectricity)* and *Electrical Circuit*. The Multiphysics coupling enables modeling both single transducer probes and phased array probes. In this study, we built a local NDI model assuming periodic

boundaries to mimic the pulse-echo-like wave propagation across transducer, wedge, adherend and adhesive. While typical NDI simulation steps in COMOSL are outlined in tutorials, e.g., the angle beam nondestructive testing example in application gallery, our simulation model is slightly different from this tutorial in physics interfaces due to the limited boundary features provided by the *Elastic Waves, Time Explicit Model*. The fracture boundary condition within the *Elastic Waves, Time Explicit* physics interface effectively simulates flaws involving material discontinuity, such as pores, small cracks, and debonding. However, it is not suitable for addressing more challenging flaws, such as the kissing bond in adhesive joints [7], which remains continuous in terms of material properties. Additionally, to the best of our knowledge, the *Elastic Waves, Time Explicit* Model physics interface does not offer periodic boundary options. Therefore, we utilized the *Solid Mechanics (Wave), Time Explicit* physics interface to define the spring-like interfacial characteristics using a thin layer boundary with spring material. Our NDI simulation is applied to aluminum lap joints. To facilitate the manipulation of simulation models for parametric studies, we used *LiveLink™ for MATLAB* to automate the pre-processing and post-processing steps in the FEA.

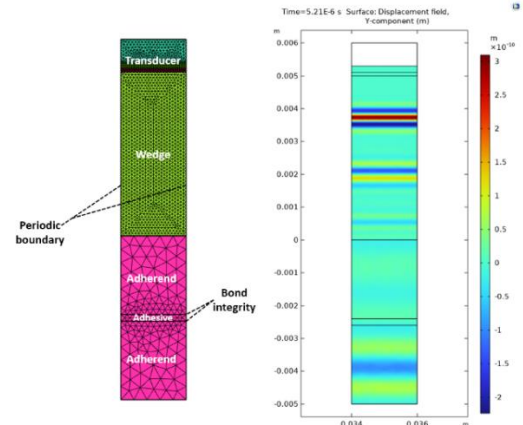


Figure 2. The NDI simulation of aluminum adhesive joint

Simulation Results & Discussion

There are two parts for simulation results, including the analysis of amplitudes of FFT for ultrasonic signals and extensive simulations with *LiveLink™*.

Part I: NDI Simulation of aluminum lap joints

The NDI simulation of aluminum lap joint is shown in Fig. 2, where the periodic boundary conditions are applied to both the left and right sides. In Fig. 2, the probe consists of a transducer and a wedge, while the adhesive joint comprises two adherends and a single adhesive layer. An absorbing layer and a matching layer are defined at the top and the bottom of the transducer, respectively. The *Electrostatics (Piezoelectricity)* and *Electrical Circuit* are defined for the middle layer of the transducer. The bond integrity is represented by the thin layer condition in

Solid Mechanics (Wave), Time Explicit Model. The width of this local model is 2 mm. The heights of transducer, wedge, adherend and adhesive are 1 mm, 5 mm, 2.4 mm and 0.2 mm, respectively. The minimum meshes sizes of different parts are determined based on their corresponding shear wave velocities. The right subplot in Fig. 2 demonstrates the displacement component u at $t = 5.21 \times 10^{-6}$ sec. In real experiments, ultrasonic couplants are used to facilitate the transmission of sound energy between transducer and wedge, wedge and adhesive joints. In our simulation, boundary pairs are used to mimic those contact boundaries. The material properties used in this paper is shown in Table 1, where c_p and c_s denote the pressure-wave and the shear-wave speed.

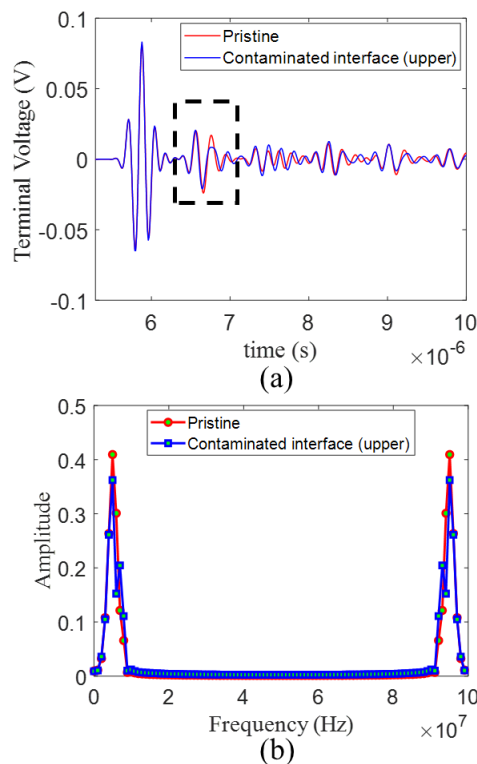


Figure 3. Ultrasound signals and FFT features

The interfacial stiffnesses K_1 and K_2 are used to access the bond integrity. Fig. 3 shows the NDI results for both pristine and contaminated adhesive joints. In the pristine adhesive joints, $K_1 = K_2 = 6$ MPa/nm, where in the contaminated joint, $K_1 = 1$ MPa/nm and $K_2 = 6$ MPa/nm. These two simulations focus solely on the spring-interface model. The study of damping parameters is discussed later in the joint simulation using MATLAB programming. Fig. 3(a) shows the ultrasound signal (i.e., A-scan signal) recorded by the transducer. Fig. 3(b) shows the FFT results corresponding to the highlighted segment in Fig. 3(a). It is observed that the contaminated interface slightly alters the shape of the A-scan signal. Once

the A-scan signals are obtained, it is crucial to choose appropriate reflection and transmission characteristics. The characteristics related to interfacial adhesion are typically, the amplitudes from FFT [5], reflection rates [1] and peak delay [6], etc. Additionally, we found that ultrasound frequency exhibits varying sensitivities to different flaws or damages; for example, 7.5 MHz is more sensitive to stiffness values between 1 and 2 MPa/nm.

Part II: Joint simulation with MATLAB programming

To facilitate multiple simulation runs, we used *LiveLink™* for *MATLAB* to automate the pre-processing and post-processing steps in FEA. The *MATLAB* codes are included in the Appendix. The spring-damper-interface is studied for the aluminum adhesive joints. In the parametric studies, the interfacial stiffness ranges from 1 MPa/nm to 6 MPa/nm, and the damping parameter ranges from 0.1 MPa/nm to 0.5 MPa/nm, assuming $D_1 = D_2$. We used reflection rate and peak delay to present the relationship between ultrasound responses and interfacial characteristics. The pristine adhesive joint without damping parameters serves as the reference simulation. Fig. 4 shows the ultrasound responses and time delay of the first 10 peaks for all simulation runs. Fig. 5 and Fig. 6 show the reflection rates and the average peak delay for different interfacial stiffnesses (K_1 , K_2) and damping parameters (D_1 , D_2). It is evident that the damping parameters cause large variance in reflection rates and peak delays. The reference [3, 6] has derived mathematical models for the reflection rates and the peak delays, but the authors only considered the spring-interface. Our simulations extend this analysis to include the spring-damper-interface model, demonstrating that the damping parameter's impact should not be overlooked, especially when damping properties are intentionally designed. The closed-form expressions derived by references [3, 6] might be modified to include damping parameters, thereby addressing a wider range of situations. Further theoretical work could be done with the current NDI simulations to explain the complex mapping relationship illustrated in Fig. 5-6. The theoretical models could then be used for fast inverse ultrasound determination^{1,8-11}. On the other hand, if the damping parameters must be ignored, the results in Fig. 5 can help account for model uncertainties.

Conclusions

COMSOL Multiphysics facilitates efficient NDI simulations by offering features such as periodic boundaries, thin layer boundaries with spring materials in *Solid Mechanics (Wave)*, and the integrated *MATLAB* simulation interface, *LiveLink™*. In our simulations, both the spring-interface and spring-damper-interface models were

Table 1: Material Properties

	Aluminum	Adhesive	Absorbing	Matching	PZT	Wedge
ρ (kg/m ³)	2700	1673	6580	2280	7500	1190
c_p (m/s)	6200	2860	1500	3400	4620	2337
c_s (m/s)	3170	1340	775	1920	1750	1157

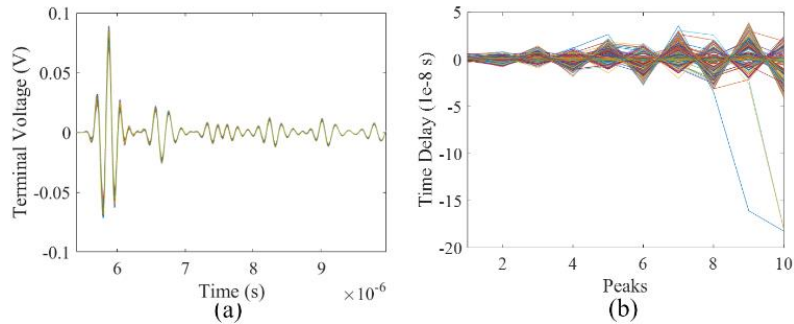


Figure 4. 180 simulation runs: (a) Ultrasound signals (b) Time delay of the first 10 peaks (100 MHz sampling rate)

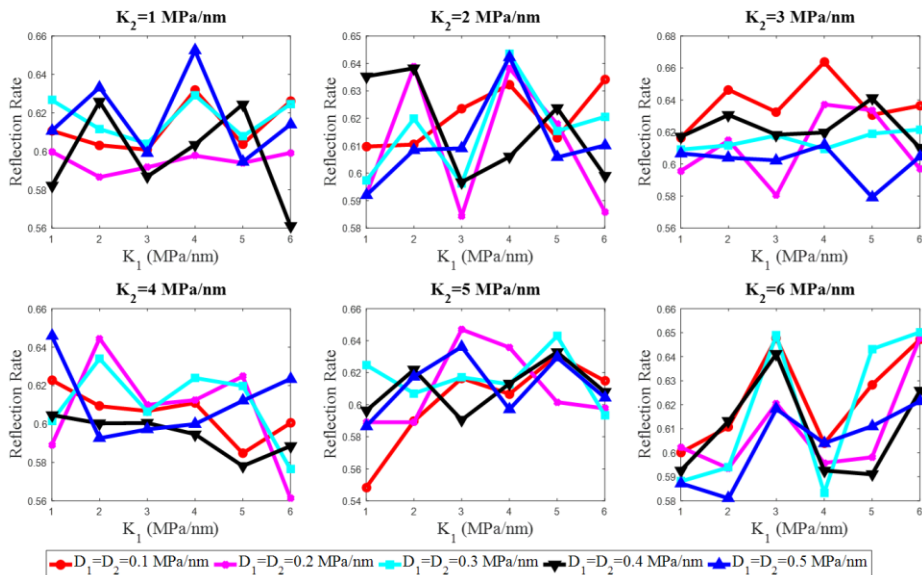


Figure 5. Reflection rates for different interfacial stiffnesses and damping parameters

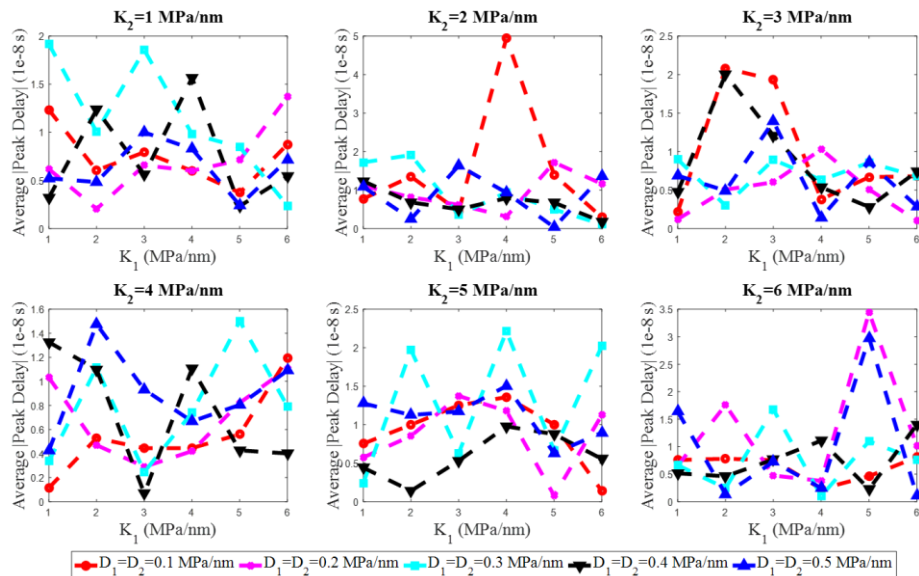


Figure 6. Average of the absolute peak delays for different interfacial stiffnesses and damping parameters (100 MHz sampling rate)

employed to capture a wider range of bonding scenarios. This study focuses on key ultrasonic reflection and transmission characteristics, including FFT amplitudes, reflection rates, and peak delays. These signal characteristics are linked to underlying interfacial parameters (K_1 , K_2 , D_1 and D_2) through physics-based numerical analysis.

Our analysis of reflection rates and peak delays reveals that the impact of interfacial damping on ultrasonic responses cannot be ignored. If the damping properties of bonding lines are attributed to flaws or damages, existing theoretical models for ultrasonic interfacial bonding evaluation may need to be revised. Otherwise, uncertainties should be factored into subsequent tasks, such as ultrasonic inverse determination. Future research could further explore the theoretical aspects of interfacial damping.

References

- [1] Matsuda, N., Mori, N., Furuta, Y., Nishikawa, M., Hojo, M., & Kusaka, T. (2019, September). Evaluation of interfacial characteristics of adhesive joints by ultrasonic reflection technique. In *Proceedings of Meetings on Acoustics* (Vol. 38, No. 1). AIP Publishing.
- [2] Golub, M. V., & Boström, A. (2011). Interface damage modeled by spring boundary conditions for in-plane elastic waves. *Wave Motion*, 48(2), 105-115.
- [3] Mori, N., Matsuda, N., & Kusaka, T. (2019). Effect of interfacial adhesion on the ultrasonic interaction with adhesive joints: A theoretical study using spring-type interfaces. *The Journal of the Acoustical Society of America*, 145(6), 3541-3550.
- [4] Tian, Y., Kim, W., Kiziltas, A., Mielewski, D., & Argento, A. (2022). Effects of interfacial dynamics on the damping of biocomposites. *Scientific Reports*, 12(1), 20042.
- [5] Roach, D., Rackow, K., & Duvall, R. (2010, June). Innovative use of adhesive interface characteristics to nondestructively quantify the strength of bonded joints. In *Proceedings of the 10th European conference on non-destructive testing, Moscow* (pp. 7-11).
- [6] Wang, X., Yao, L., Huang, Z., Ma, C., Zhang, L., Wu, N., ... & Chang, J. (2019). Evaluating interfacial bonding characteristics of the composite material thin layer by ultrasound delay time spectrum. *Composite Structures*, 222, 110913.
- [7] Jeenjitkaew, C., & Guild, F. J. (2017). The analysis of kissing bonds in adhesive joints. *International Journal of Adhesion and Adhesives*, 75, 101-107.
- [8] Yong-An, L., Jie, M., Ming-Xuan, L., Xiao-Min, W., Zhi-Wu, A., & Qiao, Z. (2010). Bonding interface imaging and shear strength prediction by ultrasound. *Chinese Physics Letters*, 27(6), 064303.
- [9] Baltazar, A., Wang, L., Xie, B., & Rokhlin, S. I. (2003). Inverse ultrasonic determination of imperfect interfaces and bulk properties of a layer between two solids. *The Journal of the Acoustical Society of America*, 114(3), 1424-1434.
- [10] Bustillo, J., Fortineau, J., Gautier, G., & Lethiecq, M. (2014). Ultrasonic characterization of porous silicon using a genetic algorithm to solve the inverse problem. *NDT & E International*, 62, 93-98.
- [11] Polihronov, Y., & Croxford, A. (2019, March). NDT assessment of bonded assemblies-image optimization for weak bond characterization using ultrasonic array transducer. In *Journal of Physics: Conference Series* (Vol. 1184, No. 1, p. 012002). IOP Publishing.

Acknowledgements

We appreciate financial support from Georgia Tech Create-X funding (2024-2025).

Appendix

Codes for running COMSOL simulations with *MATLAB*

```

% ModelUtil.showProgress(true)
model = mphopen('filename.mph');
model.study('std1').feature('time').set('tlist', 'range(0, T0/5, 50*T0)');
for kk = 1:6
    for ii = 1:6
        for jj = 1:5
            model.param.set('kk',string(kk));
            model.param.set('ii',string(ii));
            model.param.set('jj',string(jj));
            model.component('comp1').physics('solid').feature('t12').feature
('spm1').set('kPerArea', {'kk*1e15' '0' '0' '0' 'kk*1e15' '0' '0' '0' 'kk*1e15'});
            model.component('comp1').physics('solid').feature('t11').feature
('spm1').set('kPerArea', {'ii*1e15' '0' '0' '0' 'ii*1e15' '0' '0' '0' 'ii*1e15'});
            model.component('comp1').physics('solid').feature('t11').feature
('spm1').feature('dmp1').active(true);
            model.component('comp1').physics('solid').feature('t12').feature
('spm1').feature('dmp1').active(true);
            model.component('comp1').physics('solid').feature('t12').feature
('spm1').feature('dmp1').set('DampPerArea', {'jj*0.1*1e15' '0' '0' '0' 'jj*0.
1*1e15' '0' '0' '0' 'jj*0.1*1e15'});
            model.component('comp1').physics('solid').feature('t11').feature
('spm1').feature('dmp1').set('DampPerArea', {'jj*0.1*1e15' '0' '0' '0' 'jj*0.
1*1e15' '0' '0' '0' 'jj*0.1*1e15'}); model.study('std1').run;
            model.result.table('tbl1').save('signal_'+string(ii)+'_'+string(jj)
+'_'+string(kk)+'.txt');
        end
    end
end

```